

Electron-spin beat susceptibility of excitons in semiconductor quantum wells

N. H. Kwong, S. Schumacher[†], and R. Binder

College of Optical Sciences, University of Arizona, Tucson, Arizona 85721, USA

(Dated: April 15, 2008)

Recent time-resolved differential transmission and Faraday rotation measurements of long-lived electron spin coherence in quantum wells displayed intriguing parametric dependencies. For their understanding we formulate a microscopic theory of the optical response of a gas of optically incoherent excitons whose constituent electrons retain spin coherence, under a weak magnetic field applied in the quantum well's plane. We define a spin beat susceptibility and evaluate it in linear order of the exciton density. Our results explain the many-body physics underlying the basic features observed in the experimental measurements.

Spurred by prospects of applications in spintronics, the long-lived electron spin coherence of excitations in semiconductor quantum wells has been undergoing intensive investigation [1, 2, 3]. Experimentally one of the most direct and convenient ways to study this spin coherence is through the measurement of its effects on the quantum well's optical response. Nonlinear optics techniques such as differential transmission (DT) and Faraday rotation (FR) of optical probes have been used for this purpose [4, 5, 6, 7]. Typically, the electron-hole excitation is produced in a pure spin state aligned with the quantum well's growth axis in the presence of a weak magnetic field applied along the well's plane (Voigt geometry, Fig. 1a). Time-resolved DT and FR signals oscillating at the electron spin Zeeman splitting frequency are then generated by probe pulses at delay times spread over hundreds of picoseconds.

While the decay of the electron spin signals is by now well understood (for a review, see e.g. [8]), other fundamental parametric dependencies are still under active investigation. Recent reports on the measurement (DT and FR) and control of electron spin coherence in a pumped population of excitons [6, 7, 9] showed intriguing dependencies on probe frequency and intensity, which could reveal important information about the nonlinear optical properties of the electron-spin coherent, but optically incoherent, excitons. The experiments have been interpreted with phenomenological models, but a microscopic theory would provide a more in-depth understanding. The purpose of this letter is to formulate a general microscopic theory of the nonlinear optical susceptibility of a quantum well which carries a population of electron-spin-coherent excitons. Valid in linear order in both the pumped exciton density and probe field amplitude, the theory clarifies the physics of time-resolved DT and FR spin beats at the low density limit.

Microscopic theories have been extensively developed for the nonlinear response of quantum wells in the ultrafast (\leq several ps) regime. In conjunction with significant experimental efforts, these theories have established exciton-exciton interactions as the primary mechanism driving nonlinear optical effects (for recent reviews, see e.g. [10, 11, 12]). In particular, the microscopic

processes underlying *exciton-spin* beats in FR signals in this regime have been discussed [13, 14]. But so far a microscopic theory of the nonlinear optics of optically dephased, electron-spin-coherent excitons on the 100 ps time scale is still absent.

We consider specifically the experimental configuration sketched in Fig. 1a. A circularly polarized, say σ_+ , pump pulse at normal incidence (along the z -axis) and spectrally close to the lowest heavy hole exciton resonance creates an interband polarization in a quantum well at low ambient temperature, e.g. 10K. Within a time scale τ_R (< 50 ps in GaAs at 10K) after the pumping, the interband polarization partially re-radiates and partially dephases and relaxes to yield a population of incoherent heavy hole excitons with a distribution of center-of-mass momentum. The hole spin inside a pumped exciton ($j_z = 3/2$ initially) decoheres also within τ_R , while the electron spin state ($s_z = -1/2$ initially) stays pure for a long time, e.g. typically hundreds of ps in GaAs quantum wells. A magnetic field applied along an axis (the x -axis)

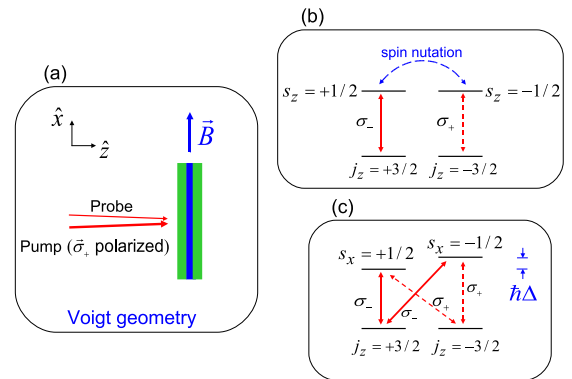


FIG. 1: (a) Sketch of the Voigt geometry with normal incidence light and a magnetic field \mathbf{B} in the quantum well plane. (b) Optical selection rules in the z -basis. The \mathbf{B} -field induced coherence between the electron states in the z -basis is indicated. (c) Optical selection rules using the z -basis for holes and x -basis (eigenstates of magnetic field Hamiltonian) for electrons.

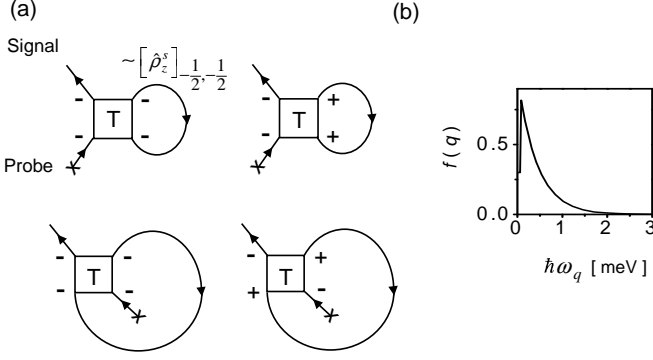


FIG. 2: (a) Diagrams representing the excitonic scattering contributions to the third order interband polarization. The internal directed line, labeled in one diagram by $[\hat{\rho}_z^s]_{-1/2, -1/2}$, represents an optically incoherent exciton. The box enclosing the letter 'T' denotes the scattering matrix or T-matrix. The electron spin states (+ or -) of the incoming and outgoing excitons of the scattering event are marked. (b) A model momentum distribution of the relaxed excitons.

in the plane of the quantum well splits the two degenerate electron spin states quantized along the x -axis (Fig. 1c) and, in the case at hand, drives a coherent oscillation of spin population between the two electron spin states quantized along the z -axis (Fig. 1b): with the electron created in $s_z = -1/2$, the electron spin density matrix in the z -axis basis is

$$\hat{\rho}_z^s(t) = \frac{1}{2} \begin{pmatrix} [1 + \cos\Delta(t - t_{\text{pu}})] & i\sin\Delta(t - t_{\text{pu}}) \\ -i\sin\Delta(t - t_{\text{pu}}) & [1 - \cos\Delta(t - t_{\text{pu}})] \end{pmatrix} \quad (1)$$

where $\hbar\Delta$ is the Zeeman splitting and t_{pu} is the pump time.

Many properties of the exciton population can be described by the one-exciton density matrix $\langle p_{\mathbf{q}}^{sj\dagger}(t) p_{\mathbf{q}'}^{s'j'}(t) \rangle$ where $p_{\mathbf{q}}^{sj}$ is the second quantized annihilation operator for a 1s heavy hole exciton with electron spin s quantized along the \hat{z} -axis, hole spin j , and center-of-mass in-plane momentum \mathbf{q} (all momenta in this paper lie in the quantum well's plane), and $\langle \cdot \rangle$ denotes an expectation value in a many-exciton state. For times larger than τ_R , when the state has decohered with respect to hole spin and momentum, the one-exciton density matrix can to a good approximation be written as an uncorrelated product of matrices in the three state labels: $\langle p_{\mathbf{q}}^{sj\dagger}(t) p_{\mathbf{q}'}^{s'j'}(t) \rangle = [\hat{\rho}_z^s]_{ss'} \delta_{jj'} \delta_{\mathbf{q}\mathbf{q}'} f(\mathbf{q})$, where $f(\mathbf{q})$ is the slowly evolving momentum distribution. The relaxation dynamics of $f(\mathbf{q})$ has previously been investigated [15]. Based on their findings, we use a model distribution, shown in Fig. 2b, which is thermal except for a radiative loss correction at low momenta.

Microscopic many-particle theory comes into play when we try to understand the measurement and manipulation of the electron spin coherence of the exciton population. Suppose a probe pulse $E_\sigma(t)$, circularly po-

larized ($\sigma = +$ or $-$) and centered spectrally at ω and temporally at t_{pr} , is sent in to measure this coherence. It does so by inducing a 1s heavy hole interband polarization which scatters off the existing spin coherent exciton population. We use real-time Green's functions and diagrammatic perturbation methods to derive equations of motion for the probe-induced interband polarization in increasing orders of the pump and probe intensities [16]. These equations are derived with electrons and holes as degrees of freedom. They are then expanded in an exciton basis and restricted to the heavy hole 1s subspace. The resulting equations – our working equations – are driven by various exciton scattering processes and Pauli blocking. (Pauli blocking turns out to be relatively unimportant here.) We illustrate the lowest order scattering processes in Fig. 2a, showing the various electron spin (in the \hat{z} -basis) combinations explicitly. In each diagram, the line starting with a cross denotes the 1s interband polarization created by the probe pulse, and the open line a propagating exciton that recombines to give the signal photon. The internal line represents a two-time correlation function of the pumped exciton population $\langle p_{\mathbf{q}}^{sj\dagger}(t) p_{\mathbf{q}'}^{s'j'}(t') \rangle = \langle p_{\mathbf{q}}^{sj\dagger}(t) p_{\mathbf{q}'}^{s'j'}(t) \rangle \exp[i\omega_q(t - t')]$, where the signs of the electron spin s and s' are marked at the line's two ends, and $\hbar\omega_q$ is the energy of the exciton with momentum \mathbf{q} . The scattering matrix [17], or T-matrix, is a ladder sum of repeated exciton interactions to all orders and so can include the process of biexciton formation. The excitonic T-matrix conserves the total electron spin of the two scattering excitons, which implies, as illustrated in Fig. 2a, that only the diagonal part of the electron spin density matrix, Eq. (1), is probed. In other words, the optical probe measures the coherent oscillation of exciton density between the two \hat{z} -quantized electron spin states.

The susceptibility for the σ -(circularly)polarized component of the probe is given by $\chi_\sigma \sim \int dt p_\sigma(t) E_\sigma^*(t)$ where $p_\sigma(t)$ is the probe-induced interband polarization. The susceptibility depends parametrically on the pump-probe delay time $\tau = t_{\text{pr}} - t_{\text{pu}}$ and the probe pulse's center frequency ω : $\chi_\sigma = \chi_\sigma(\omega, \tau)$. It gives the time-resolved FR of an x -polarized probe and the DT of a σ -polarized probe as [14] $\theta(\omega, \tau) \sim \text{Re}[\chi_-(\omega, \tau) - \chi_+(\omega, \tau)]$ and $\Delta T_\sigma(\omega, \tau) \sim -\text{Im}[\chi_\sigma(\omega, \tau)]$ respectively. We have calculated the susceptibility to linear order in the pump-induced density, which we call the third order susceptibility $\chi_\sigma^{(3)}(\omega, \tau)$. Within our theory, it can be written in the form

$$\chi_\pm^{(3)}(\omega, \tau) = C(\omega) \pm D_{\text{spin}}(\omega) \cos\Delta\tau \quad (2)$$

The response signals are similarly parameterized: $\theta(\omega, \tau) = A_\theta(\omega) \cos\Delta\tau$, $\Delta T_\pm(\omega, \tau) = A(\omega) \pm A_T \cos\Delta\tau$, with the amplitudes given by $A_\theta(\omega) \sim -\text{Re}D_{\text{spin}}(\omega)$, $A_T(\omega) \sim -\text{Im}D_{\text{spin}}(\omega)$, and $A(\omega) \sim -\text{Re}C(\omega)$. The probe pulses we use have durations of several ps, which is

long compared to the scattering duration (typically < 1 ps in GaAs) but short compared to the spin beat period (~ 70 ps in the cited experiments). It is then instructive to approximately treat the probe pulse as a continuous wave in the scattering calculation and the oscillating

electron spin population as frozen within the duration of $p_{\sigma}^{(3)}(t)$. Solving the $p_{\sigma}^{(3)}$ equation in this approximation, we obtain the ω -dependent coefficients of $\chi_{\sigma}^{(3)}$ as

$$C(\omega) \sim \sum_{\mathbf{q}} \frac{f(\mathbf{q})}{(L(\omega))^2} \left[-T_{\mathbf{q}/2, \mathbf{q}/2}^{\pm\pm}(\Omega_{\mathbf{q}}, \mathbf{q}) - T_{\mathbf{q}/2, -\mathbf{q}/2}^{\pm\pm}(\Omega_{\mathbf{q}}, \mathbf{q}) - T_{\mathbf{q}/2, \mathbf{q}/2}^{\pm\mp}(\Omega_{\mathbf{q}}, \mathbf{q}) + \frac{1}{2} T_{\mathbf{q}/2, -\mathbf{q}/2}^{\pm\mp}(\Omega_{\mathbf{q}}, \mathbf{q}) + (\tilde{A}_e^{\text{PSF}}(\mathbf{q}) + \tilde{A}_h^{\text{PSF}}(\mathbf{q}))L(\omega) \right] \quad (3)$$

$$D_{\text{spin}}(\omega) \sim \sum_{\mathbf{q}} \frac{f(\mathbf{q})}{(L(\omega))^2} \left[-T_{\mathbf{q}/2, \mathbf{q}/2}^{\pm\pm}(\Omega_{\mathbf{q}}, \mathbf{q}) + T_{\mathbf{q}/2, \mathbf{q}/2}^{\pm\mp}(\Omega_{\mathbf{q}}, \mathbf{q}) - \frac{1}{2} T_{\mathbf{q}/2, -\mathbf{q}/2}^{\pm\mp}(\Omega_{\mathbf{q}}, \mathbf{q}) + \tilde{A}_e^{\text{PSF}}(\mathbf{q})L(\omega) \right] \quad (4)$$

Here $T_{\mathbf{k}_f \mathbf{k}_i}^{\sigma\sigma'}(\Omega, \mathbf{Q})$ denotes a two-exciton scattering (or T-matrix) element [17] between an incoming state with relative momentum \mathbf{k}_i and an outgoing state with relative momentum \mathbf{k}_f , and $\hbar\Omega$ and \mathbf{Q} are the conserved total energy and momentum respectively. The superscripts σ, σ' label the polarization channel: $T^{++}(=T^{--})$ is the T-matrix for co-polarized excitons, and $T^{+-}(=T^{-+})$ is that for counter-polarized excitons. For each process both the incoming and outgoing states contain a virtual (probe) exciton with zero momentum and energy $\hbar\omega$ and a real (pump) exciton with momentum \mathbf{q} and energy $\hbar\omega_q = \varepsilon_x + \hbar^2 q^2 / (2M_x)$, M_x being the exciton's mass. These give a total energy of $\Omega_{\mathbf{q}} = \omega + \omega_q$ and a total momentum of \mathbf{q} . $L(\omega) = \hbar\omega - \varepsilon_x + i\gamma$ where γ is the linewidth of the exciton resonance. The phase space filling factors are given in terms of the momentum space 1s exciton wavefunction $\phi(\mathbf{k})$ by $\tilde{A}_{\alpha}^{\text{PSF}}(\mathbf{q}) = \sum_{\mathbf{k}} \phi(\mathbf{k}) |\phi(\mathbf{k}_{\alpha})|^2 / \sum_{\mathbf{k}} \phi(\mathbf{k})$, where $\mathbf{k}_{\alpha} = \mathbf{k} - (m_{\alpha}/M_x)\mathbf{q}$, with $\alpha = e, h$. The T-matrix elements are calculated by diagonalization of the two-exciton Hamiltonian as explained in [17].

Equation (2) shows a simple dependency to pump-probe polarization configurations: the co-polarized (+ pump and + probe) and counter-polarized (+-) response signals share a common τ -independent part but have 180°-out-of-phase spin beat parts. At the same time, Eqs. (3) and (4) show that, even for the co-polarized configuration, say, both T^{++} and T^{+-} contribute. In particular, biexciton formation, present in T^{+-} , plays a part in the co-polarized channel response. Moreover, Eq. (2) shows that the non-beat part of the FR of a linearly-polarized probe vanishes. These properties follow from our assumption of hole spin thermalization, which produces all four exciton (s_z, j_z) spin states in the relaxed exciton population even though the pump is circularly polarized. These polarization dependencies are in ob-

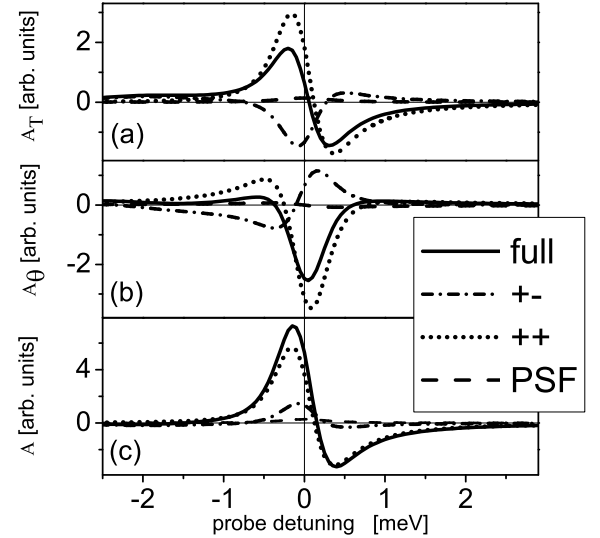


FIG. 3: (a) and (b). The (signed) amplitudes of the electron spin beat signals of a GaAs quantum well as a function of probe frequency for a (+)-polarized pump: (a) differential transmission (DT) of a (+)-polarized probe and (b) Faraday rotation (FR) of a linearly polarized probe. (c) The non-beat part of the DT. Also shown is the breakdown of each signal into its components: phase space filling (dashed), exciton scatterings T^{++} (dotted) and T^{+-} (dash-dotted).

vious contrast to those of the $\chi^{(3)}$ susceptibility in ultrafast pump-probe spectroscopy (e.g. [18]), where $T^{\sigma\sigma'}$ contributes only in the matching ($\sigma\sigma'$) pump-probe polarization channel, yielding distinctly different responses in the (++) and (+-) pump-probe configurations [19].

We have calculated $C(\omega)$ and $D_{\text{spin}}(\omega)$ for the exci-

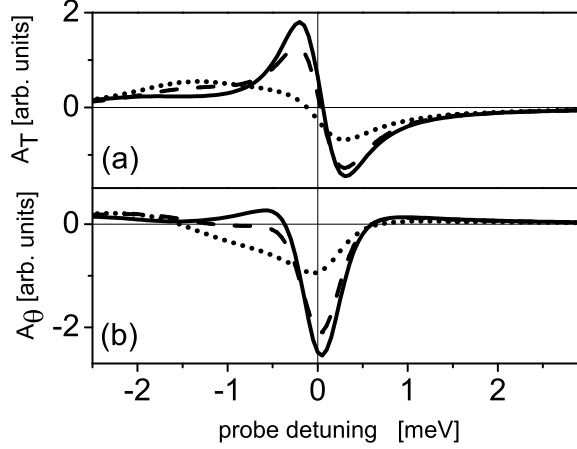


FIG. 4: Sensitivity of the electron spin beat signals to variations in the strength and/or resonance energy of the bound biexciton. Solid: same as solid curves in Fig. 3, for which the biexciton binding energy ε_{bx} is calculated to be 1.8 meV. Dashed: ε_{bx} is shifted to 1.3 meV, other components being the same as for the solid curves. Dotted: ε_{bx} is shifted to 1.3 meV, and biexciton strength is raised by a factor of 1.5.

ton momentum distribution shown in Fig. 2b, with an exciton linewidth of $\gamma = 0.35$ meV and a biexciton dephasing of 2γ . In our calculation, the $p_{\sigma}^{(3)}(t)$ equation is solved with 4-ps probe pulses, i.e., without assuming the probe to be a continuous wave. The effect of the 'continuous-wave' approximation is, however, small so that Eqs. (3) and (4) can be used to interpret the numerical results. Fig. 3 shows (a) the spin beat amplitude $A_T(\omega)$ of the DT of a (+)-polarized (co-polarized with the pump) probe, (b) the beat amplitude $A_{\theta}(\omega)$ of the FR of a linearly polarized probe, and (c) the non-beat part $A(\omega)$ of the DT. The signals' spectral behaviors are basically products of those of the T-matrix elements and one-exciton Lorentzians $[L(\omega)]^{-2}$. The spectra of our finite- \mathbf{q} T-matrix here are qualitatively similar to those of the zero- \mathbf{q} T-matrix for ultrafast nonlinear optics discussed in [17]. A prominent feature in Fig. 3 is the considerably larger magnitude of the non-beat part of the DT signal compared to A_T and A_{θ} . This can be understood from the breakdown into contributions from various processes, also shown in the figure. For the spin beat amplitudes, the contributions from T^{++} (dotted lines) and T^{+-} (dash-dotted lines) largely counteract each other, especially near the exciton resonance ($\hbar\omega \approx \varepsilon_x$). This effect can be expected from the opposite signs with which the two contributions appear in Eq. (4) for $D_{\text{spin}}(\omega)$. In contrast, as seen from Eq. (3), T^{++} and T^{+-} tend to reinforce each other in $C(\omega)$, which also contains an extra $T_{\mathbf{q}/2, -\mathbf{q}/2}^{++}$.

The smallness of A_T relative to the non-beating part of the DT signal is in accord with experimental measurements of DT, especially around zero probe detuning [6, 7]. The relative phase ($= 180^\circ$) between the beats in the DT in the two pump-probe polarization configurations is also confirmed [20]. The ω -dependence of A_{θ} shown in Fig. 3 also agrees qualitatively with measurements [7]. We note that our theory is essentially parameter-free (the input parameters being the electron and hole masses, the background dielectric constant, and environmental dephasings) with a model of a zero-width quantum well with two bands. Bearing this model's limitations in mind, we think the general agreement between our predictions and experiments is sufficient to validate the physical points of our theory. More accurate modeling of the experimental samples, such as including effects of a finite well width and the light hole band, will be done in the future. To get a rough sense of how these modeling advances might change our results, we have repeated our calculations, artificially varying the biexciton energy and strength from their calculated values. These biexciton characteristics are known to depend quite sensitively on the well width. From Fig. 4, one can see the qualitative features of our theory are robust, but improved sample modeling would be needed for precise predictions.

In summary, we have formulated a microscopic theory, based on exciton interactions, for the electron spin beat components of differential transmission and Faraday rotation signals of quantum wells carrying a population of dephased, but electron spin coherent excitons. This theory explains the basic features of recent experimental results at the limit of low pump-induced density and low probe intensity. The theory will be generalized to higher orders in the probe intensity and to three-pulse configurations [9].

We thank H. Wang, Y. Shen, and S. O'Leary for valuable discussions and JSOP for financial support. S. Schumacher gratefully acknowledges financial support by the DFG (SCHU 1980/3-1).

[†] Present address: Physics Department, Heriot-Watt University, Edinburgh EH14 4AS, UK

-
- [1] S. A. Wolf *et al.*, Science **294**, 1488 (2001).
 - [2] D. D. Awschalom, M. E. Flatté, and N. Samarth, Sci. Am. **0602**, 67 (2002).
 - [3] W. H. Lau, J. T. Olesberg, and M. E. Flatté, Phys. Rev. B **64**, 161301(R) (2001).
 - [4] J. M. Kikkawa and D. D. Awschalom, Phys. Rev. Lett. **80**, 4313 (1998).
 - [5] N. Samarth, *Solid State Physics v. 58* (Elsevier, Amsterdam, 2004), pp. 1–72.
 - [6] P. Palinginis and H. Wang, Phys. Rev. Lett. **92**, 037402 (2004).
 - [7] Y. Shen *et al.*, Phys. Rev. B **72**, 233307 (2005).

- [8] I. Žutić, J. Fabian, and S. das Sarma, Rev. Mod. Phys. **76**, 323 (2004).
- [9] Y. Shen, A. M. Goebel, and H. Wang, Phys. Rev. B **75**, 045341 (2007).
- [10] D. Chemla and J. Shah, Nature **411**, 549 (2001).
- [11] V. M. Axt and T. Kuhn, Rep. Prog. Phys. **67**, 433 (2004).
- [12] T. Meier, P. Thomas, and S. Koch, *Coherent Semiconductor Optics* (Springer, New York, 2006).
- [13] T. Östreich, K. Schönhammer, and L. J. Sham, Phys. Rev. Lett. **75**, 2554 (1995).
- [14] L. Sham, Journal of Magnetism and Magnetic Materials **200**, 219 (1999).
- [15] C. Piermarocchi *et al.*, Phys. Rev. B **53**, 15834 (1996).
- [16] N. H. Kwong and R. Binder, Phys. Rev. B **61**, 8341 (2000).
- [17] R. Takayama *et al.*, Eur. Phys. J. B **25**, 445 (2002).
- [18] R. Takayama *et al.*, J. Opt. Soc. Am. B **21**, 2164 (2004).
- [19] C. Sieh *et al.*, Phys. Rev. Lett. **82**, 3112 (1999).
- [20] Y. Shen and H. Wang, 2007, private communication.